Covaris®
a PerkinElmer Company

Optimizing Automated Sample Preparation with Adaptive Focused Acoustics® (AFA®) for Proteomics of Human Adipose Tissue

Magdalena Perczak[1], Luojiao Huang[1], Pieter Emans[1], Sameer Vasantgadkar[2], Debadeep Bhattacharyya[2], Akshay Dhingra[2], and Berta Cillero-Pastor[1]

1 - Maastricht University, 6211 LK Maastricht, Netherlands and 2 - Covaris, LLC, Woburn, MA 01801, United States

Introduction

In bottom-up proteomics, proteins are enzymatically digested into peptides prior to final mass spectrometry for identification, characterization, or quantitation.[1] Typically, the workflow consists of multiple sample preparation steps: protein extraction, purification, digestion, separation with liquid chromatography (LC), and ion fragmentation with tandem mass spectrometry (MS/MS), referred to as LC-MS/MS.[2] Such an approach can be particularly useful for discovery and quantification of biomarkers, which are proteins that could give insights into pathogenesis of certain diseases such as osteoarthritis (OA).[3] OA is characterized by cartilage damage and bone remodeling resulting in pain, stiffness, and limited joint function.[4] It is thought that the infrapatellar fat pad, also known as Hoffa's fat pad (HFP), located in the knee, is playing a main role in OA development.[5] Although OA is a commonly occurring condition among the elderly population, it is challenging to detect it before the first symptoms appear, as there are no characterized biomarkers that could enable early diagnosis.[4,5]

From characterization to quantitation in bottom-up proteomics, sample preparation is one of the most crucial steps. Traditional tissue protein extraction usually involves manual or mechanical tissue homogenization with a lysis buffer, followed by freeze-thawing or sonication. This comes with various challenges such as incomplete lysis, contamination during sample handling, uncontrolled degradation of proteins, and sample heterogeneity that can easily introduce bias.[6] Poor reproducibility is particularly a limitation in studies investigating low-abundance proteins.[7,8] These low-abundance proteins may provide valuable insights into disease pathogenesis, highlighting the importance of developing strategies to overcome the challenges associated with their detection and analysis.[9]

To overcome these limitations, Covaris Adaptive Focused Acoustics (AFA) provides a high-throughput extraction approach using the R230 Focused-ultrasonicator.[10] This system uses non-contact, focused acoustic energy to process samples in sealed vessels, eliminating cross-contamination. By utilizing short wavelengths, it maximizes energy efficiency while minimizing heat, ensuring high protein yields and sample integrity. Ultimately, this technology delivers faster, more reproducible results with less manual handling than traditional methods.[11]

AFA technology was reported to offer promising results and facilitate sample preparation for proteomics studies. This work aims to investigate the performance of the automated protein extraction using AFA technology and assess the protein coverage on Hoffa's fat pad from OA patients with MS-based proteomics analysis.

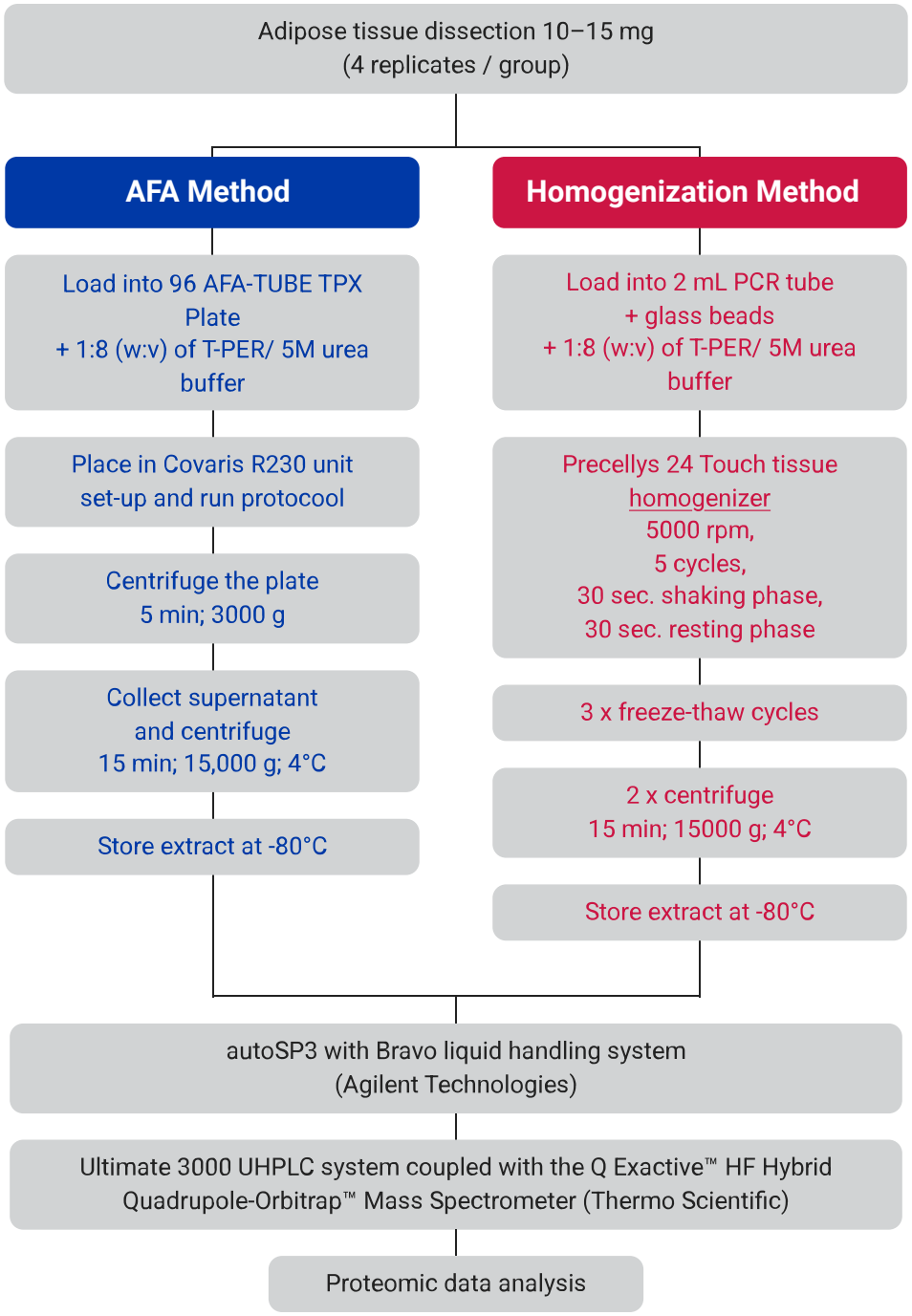


Figure 1. Overview of the workflow for AFA and homogenization methods.

1. Protein Extraction

HFP samples from waste material, were freshly collected (with ethical approval) from patients who underwent knee surgery at Maastricht University Medical Center+ with number MEC 2017–0183. Tissue samples were immediately snap-frozen using liquid nitrogen and later stored at -80°C until analysis.

To determine whether AFA improves protein extraction of adipose tissue proteins, we performed human Hoffa's fat pad protein extraction with two different methodologies. Homogenization method was performed with mechanical tissue homogenization using the Precellys 24 Touch tissue homogenizer (Bertin Technologies) combined with freeze-thawing.[12,13] AFA method was performed using the R230 Focused-ultrasonicator.[10,14] Frozen tissue was dissected on dry ice into four replicate pieces of 10–15 mg each. For homogenization method, samples were placed into 2 mL PCR tubes loaded with 20 glass beads (1 mm). For AFA method, samples were placed into wells of a 96 AFA-TUBE TPX Plate. Every sample was mixed with the extraction buffer at a 1:8 tissue-to-buffer ratio (w:v). Two types of extraction buffer were used in this study: urea (5M in 50 mM ammonium bicarbonate) and T-PER™ Tissue Protein Extraction Reagent buffer (Thermo Fisher Scientific, United States).[13,14] 5M urea was always freshly prepared before sample extraction.

For the homogenization method, the parameter settings used on Precellys were 5000 rpm, 5 cycles, each cycle with 30 sec. shaking phase, 30 sec. resting phase. After briefly spinning down the sample, three freeze-thaw cycles were performed using liquid nitrogen and water bath sonication. Samples were centrifuged for 15 min at 15,000 g at 4°C twice for liquid layer collection.[13,15]

For AFA method, different AFA settings were selected based on literature, and setting limits were tested to see whether modifying the acoustic energy affects the extraction efficiency (**Table 1**).[16,17] The "Reference 20°C" was selected as starting point. After running the AFA protocol, the plate was centrifuged for 5 min at 3000 g. The supernatant was transferred to a new Eppendorf tube and centrifuged again for 15 min at 15,000 g at 4°C for liquid layer collection.[14] All protein extracts were stored at -80°C and later measured using the Bradford assay (Bio-Rad Laboratories) for total protein estimation.[10]

Table 1. Different Covaris R230 Focused-ultrasonicator protocol settings.

Protocol	Reference	Method 1	Method 2	Method 3	Method 4	Method 5	Method 6	Method 7	Method 8
Temp (°C)	6 / 20	6 / 20	6 / 20	6 / 20	6 / 20	6	6	6	6
Peak Power (W)	350	125	350	350	350	350	125	350	350
Duty Factor (%)	25	25	32	25	25	25	32	25	25
Cycles per Burst	200	200	200	500	200	800	200	500	800
Time (sec)/Cycle	60	60	60	60	60	60	60	60	60
Number of Cycles	5	5	5	5	15	5	5	15	15

2. Proteomics

Based on the results of total protein estimation, three replicates were chosen for proteomics analysis using LC-MS/MS. An automated single-pot solid-phase-enhanced sample preparation, referred to as autoSP3, was carried out on the Bravo liquid handling system (Agilent Technologies) for protein digestion.[18] Based on the lowest concentration in the cohort, samples were diluted to a constant concentration of 0.6 mg/mL, and loaded into a 96-well plate.[19] To obtain the reducing agent, 78.8 mg of DL-Dithiothreitol (DTT) (Sigma-Aldrich) was dissolved in 800 µL of 50 mM ABC (634.5 mM DTT solution). For the alkylating agent, 75 mg of iodoacetamide (IAM) (Sigma-Aldrich) was dissolved in 400 µL of 50 mM ABC. Briefly, each sample was treated with 10 µL reductant reagent and incubated 45 min at room temperature, then alkylated with 5 µL acetylation reagent for 45 min at room temperature. Paramagnetic beads were used following supplier's recommendations, at a 1:10 protein/bead ratio (Sigma-Aldrich).[19] For protein digestion, Trypsin/Lys-C Mix Mass Spec Grade (Thermo Scientific) was prepared in a 1:25 enzyme/protein ratio with 50 mM ABC.[20] Digestion was finally quenched by 5% trifluoroacetic acid in ACN. Samples were transferred to a 1.5 mL Eppendorf tube and centrifuged for 30 min at 15,000 g at 4°C.[21] 60 µL of each sample were transferred to glass vials; these samples were ready for LC-MS analysis.

An Ultimate 3000 UHPLC system (Thermo Scientific) coupled with the Q Exactive™ HF Hybrid Quadrupole-Orbitrap™ Mass Spectrometer (Thermo Scientific) was employed. Samples were separated over phase A (100% water + 0.1 % formic acid) and phase B (ACN + 0.1 % formic acid) with a 60-minute linear gradient (5%–40% solvent B, flow rate 300 nL/min). The instrument was set to positive polarity with 385 to 1015 mass-to-charge ratio (m/z) with 60,000 resolution data-independent acquisition (DIA) mode.[13]

DIA-NN software (version 1.9.2) was used for proteomics data processing[22,23] with FASTA file Homo sapiens (Tax ID 9606) from UniProt database (7–30 peptide length range; 1–4 precursor charge range; 385–1015 precursor m/z range; 200–1800 fragment m/z range; in-silico digestion with trypsin/lysC, a maximum of 1 missed cleavage sites; N-terminal methionine excision enabled and cysteine carbamidomethylation as a fixed modification; FDR≤ 1%).[24,25] The obtained matrix was then imported into the Perseus software, where we performed statistical analysis, student's t-test and Benjamini-Hochberg, to examine whether changing AFA settings affects the proteome outcome and which method was more suitable for low abundance proteins. Gene ontology (GO) enrichment analysis for differential proteins was analyzed with the ShinyGO tool.

3. Results

Comparison of Total Protein Extraction

A 1:8 tissue-to-buffer ratio was employed using a 96 AFA-TUBE TPX Plate. Regarding the different AFA methods and the effect on extracts' concentration, we observed that the choice of extraction buffer had the highest effect, as generally T-PER resulted in higher concentrations of extracted proteins compared to 5M urea (**Figure 2**). Additionally, when comparing the temperature effect, we observed that lowering the temperature generally increased the concentration in urea samples.

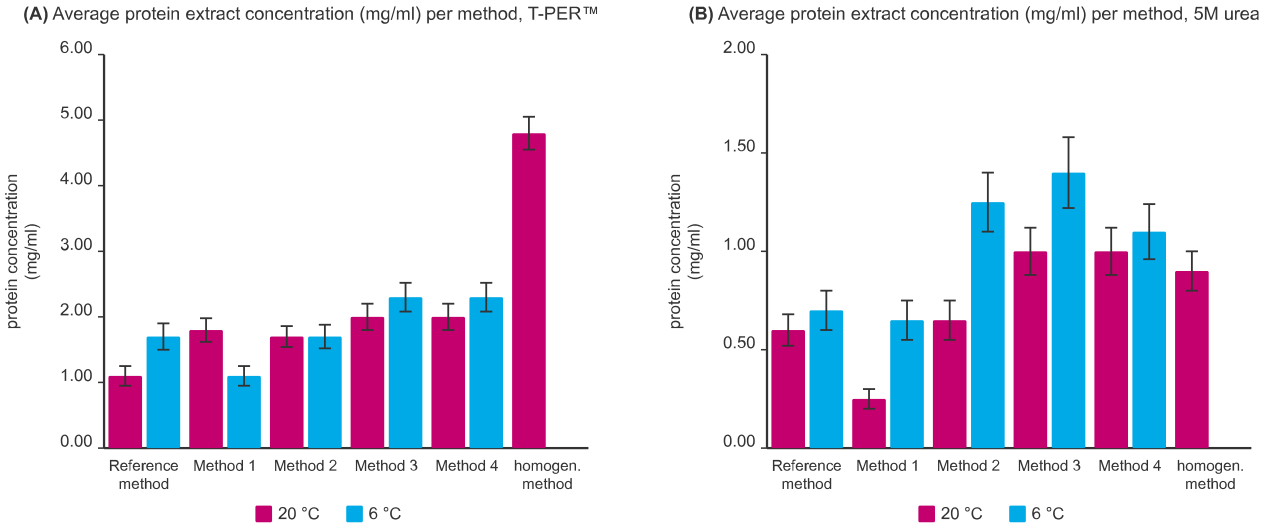


Figure 2. The effect of AFA extraction temperature on average concentration (mg/ml) of protein extracts in T-PER (**A**) and 5M urea (**B**).

Further AFA extractions were thus performed at 6°C, as lower temperature enhanced urea's stability and improves protein extraction.[26] Only the "Reference method" was carried out at both 6°C and 20°C. Another setting in the AFA method group was included, "Method 5", where we increased "cycles per burst" value to its maximum of 800. After repeating the extraction, keeping both 6°C and 20°C for the Reference method, we could see similar trends (**Figure 3**).

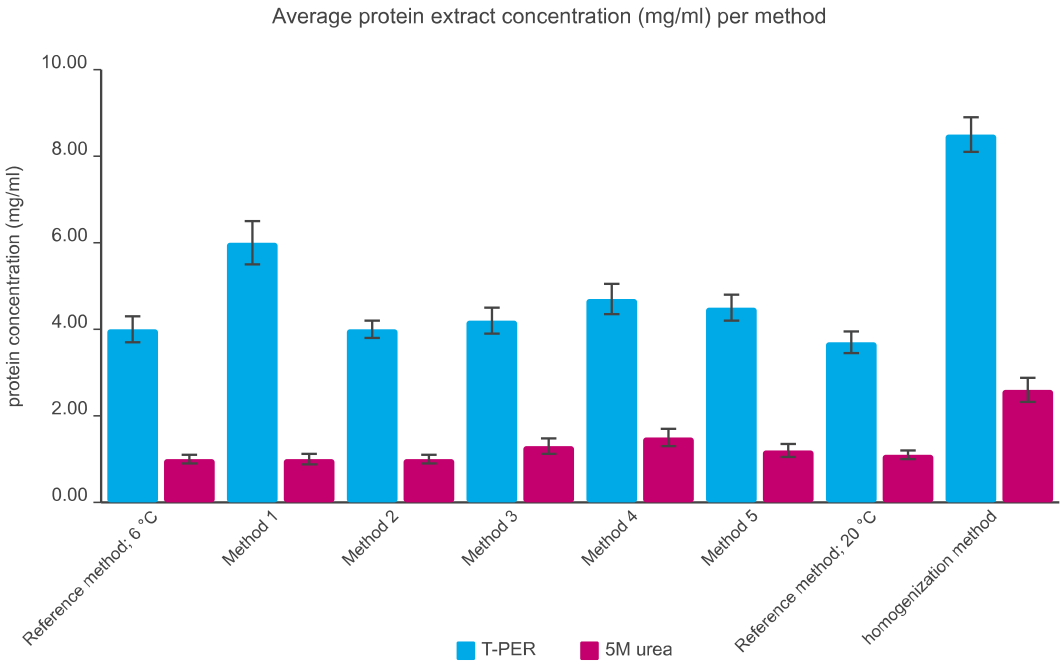


Figure 3. Protein extraction average concentration (mg/ml) per extraction method; T-PER™ buffer and 5M urea buffer.

We were again able to reach higher concentrations with T-PER buffer compared to 5M urea buffer. In both buffer groups, the homogenization method, however was able to reach higher concentrations compared to AFA method.

In the final extraction experiment on white adipose tissue samples, we have combined the AFA settings from different methods. "Method 6", as a combination of methods 1 and 2; "Method 7" as a combination of methods 3 and 4; and "Method 8" as a combination of methods 4 and 5.

In the AFA method group some settings tended to give a higher concentration yield throughout the experiments, however usually those differences were not statistically significant (**Figure 4**).

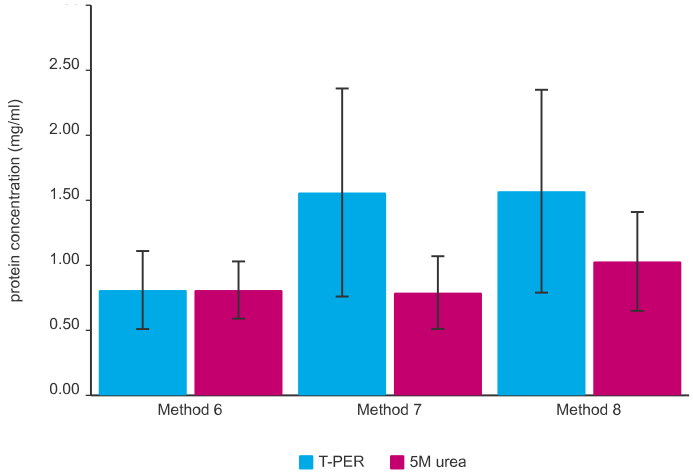


Figure 4. Average protein concentration in samples treated with T-PER™ and 5M urea buffer (carried out at 6°C).

Extracted Proteome Comparison

In proteomics workflows the performance of a sample preparation method is not primarily evaluated based on total protein yield, but rather on the depth of proteome coverage and the ability to detect proteins present at low abundance levels. Next, we investigated proteome differences between samples treated with different AFA settings to determine whether a specific protocol for AFA (**Table 1**) improved the protein extraction in terms of numbers and type of proteins. Although variable yields were observed from different protein extractions, this did not affect a comparable proteomic analysis, as the samples were brought to equal concentrations before protein digestion. The PCA plot showed a clear clustering between the two buffers with a separation over the "Component 1 axis" (**Figure 5**). The heatmap analysis further showed this clear distinction between the two buffer groups (**Figure 6**). The choice of buffers showed the biggest effect on protein extraction. The manufacturer has described T-PER as a mild reagent with a neutral pH, and it is typically recommended for fibrous and collagenous tissues.[27]

To evaluate the impact of different AFA settings on protein extraction, we further compared the protein count and type detected among samples treated with the same lysis buffer. No significant differences in protein counts were observed across protocols. In TPER-treated samples, only three protein IDs with adjusted p-values below 0.05 showed differences, whereas none did in samples treated with urea (**Table 2**). This suggested that changing the acoustic energy input does not influence the protein extraction to a significant level. For this reason, for further analysis, we only compared the homogenization method with the samples extracted with AFA method using the protocol of "Reference at 6°C".

Table 2. Differences between proteins identified in different AFA extraction methods in T-PER (in format Reference vs method).

Method	Protein Group	Protein Names	Protein Description	q-values	Mean Difference
Reference vs Method 6	Q99497 Q9BUF5	PARK7_HUMAN TBB6_HUMAN	Parkinson disease protein 7 Tubulin beta-6 chain	0.044 0.044	6 - 0.497 - 1.022
Reference vs Method 3	P25311	ZA2G_HUMAN	Zinc-alpha-2-glycoprotein	0.047	- 0.4

***Note:** Only groups that showed differences are shown in the table.

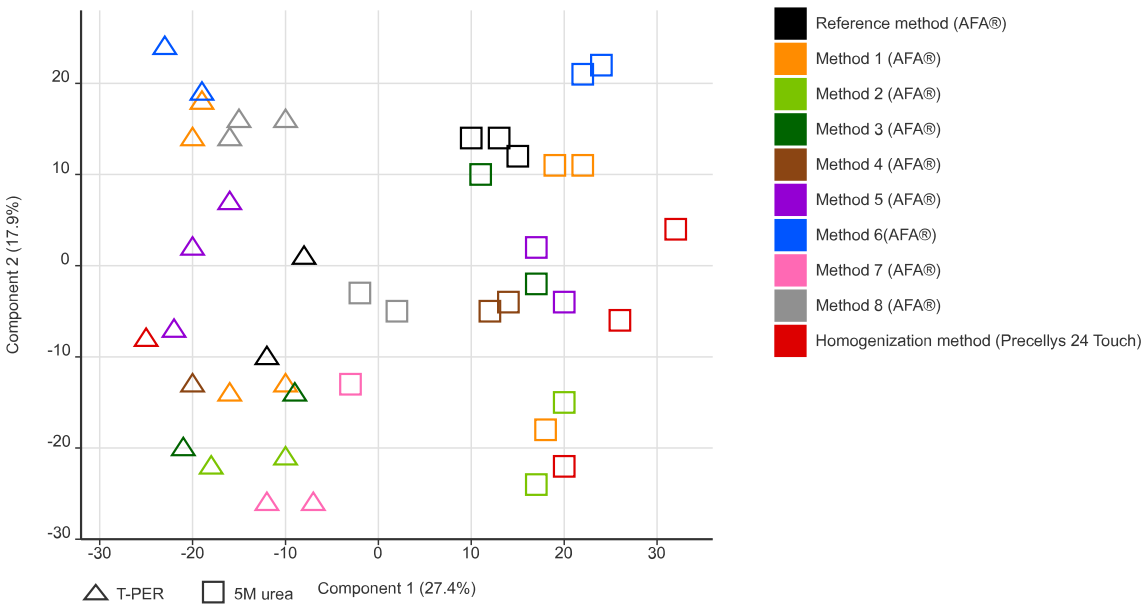


Figure 5. PCA plot of different protein extraction groups, experimental or homogenization method, in T-PER (triangles) or 5M urea buffer (squares).

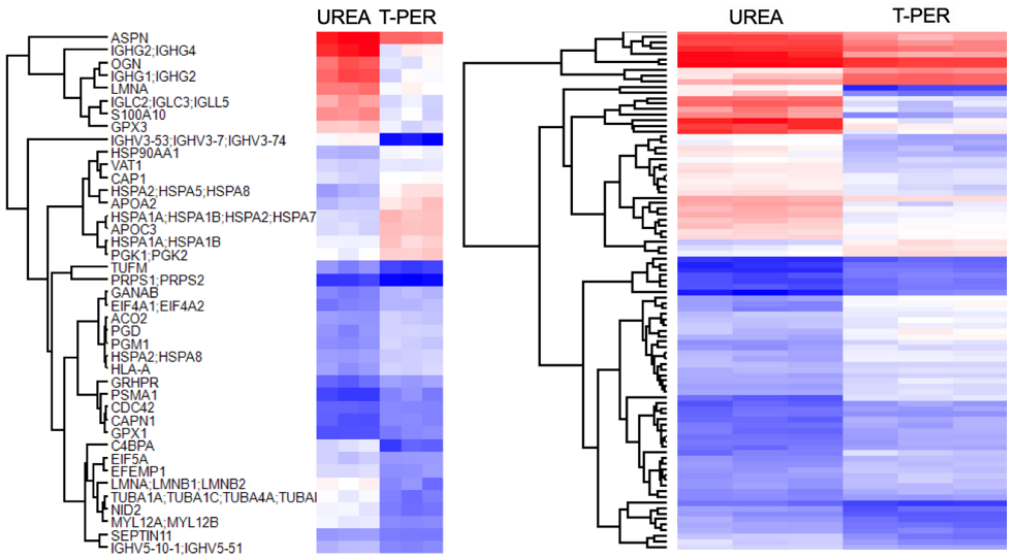


Figure 6. Heatmap analysis of method homogenization/Precellys (left) and method AFA (right) of T-PER and 5M urea buffer, where: red - high intensity, blue - low intensity.

As shown in **Table 3**, method AFA with "Reference" protocol using both buffers obtained similar protein IDs. In comparison, the method homogenization obtained 1377 and 1480 protein IDs using T-PER and 5M urea, respectively. Although the AFA method yielded a lower total protein extraction than the homogenization method, it allowed a higher number of identified protein species.

Moreover, we investigated the proportion of low-abundance proteins among all detected protein species to check whether more protein ID signals with low signal intensity were detected using AFA. We defined low-abundance proteins as those with abundances below 25% of the highest protein abundance in the entire sample matrix.[28] Each protein had to be detected in at least two out of three replicates to be qualified for low-abundance count. Statistical analysis showed that the number of protein IDs was higher with the AFA method compared to homogenization method (**Table 3**). This gave us an indication that AFA method can be more beneficial for low-abundance protein extraction; however further research would have to investigate whether these proteins are present in low concentrations in the sample. Additionally, we observed that the 5M urea buffer identified more low-abundance proteins compared to T-PER, even though previous results showed 5M urea buffer achieved a lower total protein yield than T-PER buffer. This suggests that buffer composition influences the proteome coverage, and that the extraction efficiency cannot be assessed solely based on the total protein yield.

Table 3. Average protein ID count in Covaris AFA (experimental) and Precellys® samples in T-PER and 5M urea buffer. Total low-abundant protein counts were calculated based on the average across triplicates.

Extraction Method	Total Protein Count (average)	Total Low-abundant Protein Count	Percentage of Low-abundant Proteins (%)
Homogenization; T-PER	1377	180	13.07
AFA; T-PER	1623	380	23.42
Homogenization; 5M urea	1480	296	20
AFA; 5M urea	1623	412	25.4

Next, we compared the protein abundance extracted by the homogenization method with the AFA method using a two-sample t-test with Benjamini-Hochberg correction. The results showed 13 proteins were observed with differences in the samples treated with the T-PER buffer, with 5 more abundant in the homogenization method and 8 in the AFA method. In the samples extracted with the 5M urea buffer, we observed significant differences in 34 proteins, with 22 more abundant in the homogenization method and 12 in the AFA method.

Samples Treated with T-PER

Five significant proteins were more abundant in the T-PER homogenization group, these proteins could be mainly found in extracellular spaces such as extracellular regions, vesicles, and extracellular organelles (**Figure 7A**). Noticeable cellular components include collagen trimers, with relatively small significance, while the highest significance of cellular components was observed in ECM structures (**Figure 7A**). The molecular function analysis showed high fold enrichment with strong significance for superoxide dismutase activity and oxidoreductase activity acting on superoxide radicals as acceptor (**Figure 7B**).[31,32] The significant proteins were mainly extracellular, ATP synthase F(1) complex subunit beta (P06576) was the exception. Examples included lumican (P51884), upregulated in OA and known for causing inflammation and cartilage degradation, or superoxide dismutase (P08294), an extracellular protein involved in ROS production.[29,30]

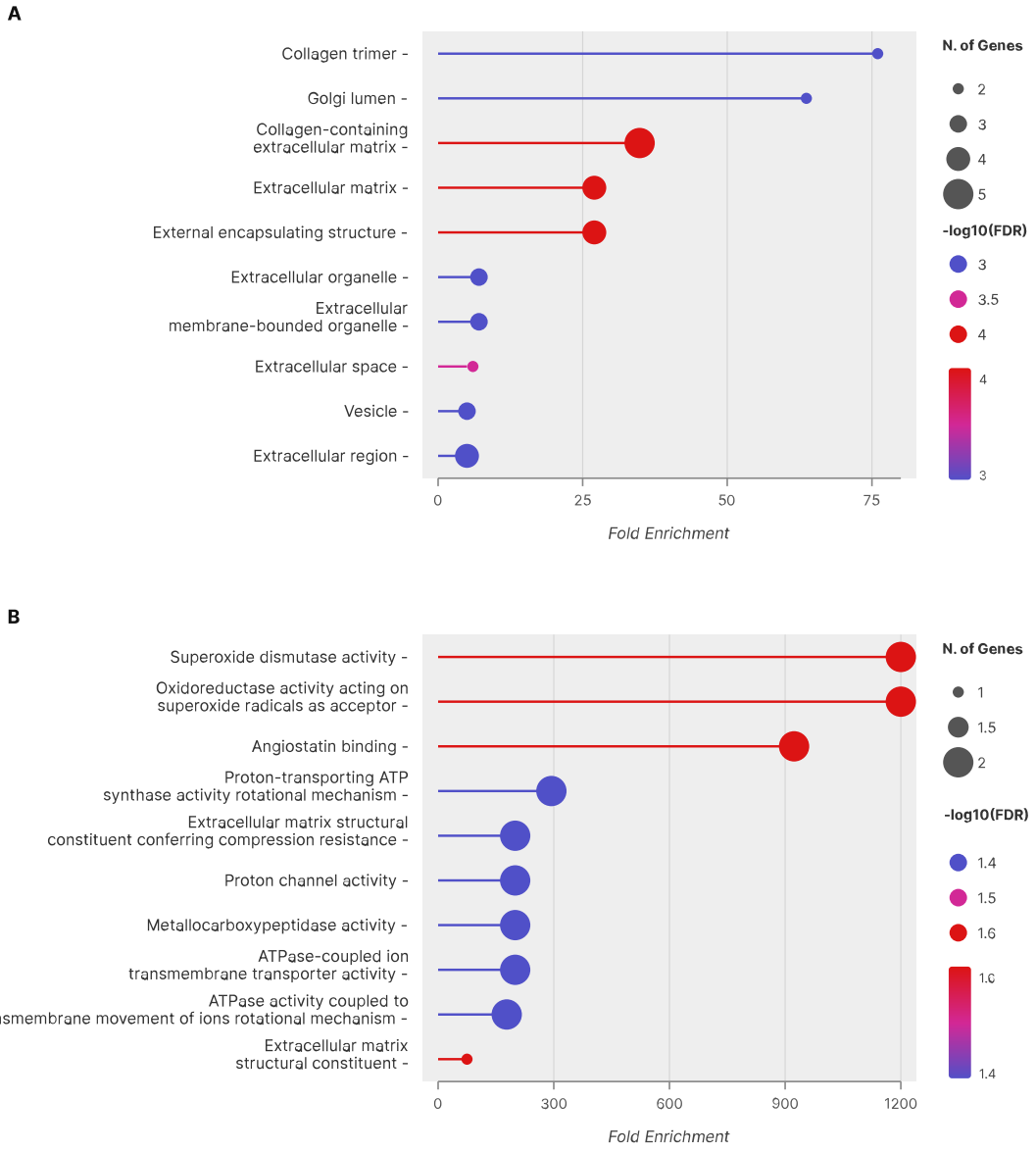


Figure 7. Fold enrichment analysis of proteins abundant in homogenization method samples with T-PER buffer, "GO Cellular component" (**A**) and "GO Molecular function" (**B**).

Eight significant proteins were more abundant in the T-PER AFA group. They were mainly found in extracellular organelles and cytoskeletal structures, and they mainly played a role in molecule binding (**Figure 8A**). The highest fold enrichment was observed for eukaryotic translation elongation factor 1 complex, also noted in the molecular function analysis, where "Translation elongation factor activity" had the highest fold enrichment (**Figure 8B**). Elongation factor 1-alpha 1 protein (P68104) is a translation elongation factor that additionally plays a role in interferon gamma transcription regulation.[31] Other identified proteins, scaffold protein ILK (Q13418), palladin (Q8WX93), and plectin (Q15149) are related to cytoskeletal structures. ILK plays a role in cell adhesion and migration, and palladin, a phosphoprotein, is required for proper assembly and remodeling of the actin cytoskeleton.[32,33] Plectin proteins are responsible for cytoskeleton crosslinking and shape the intermediate filaments within the cytoplasm, having a direct effect on tissue architecture and mechanical stability.[34]

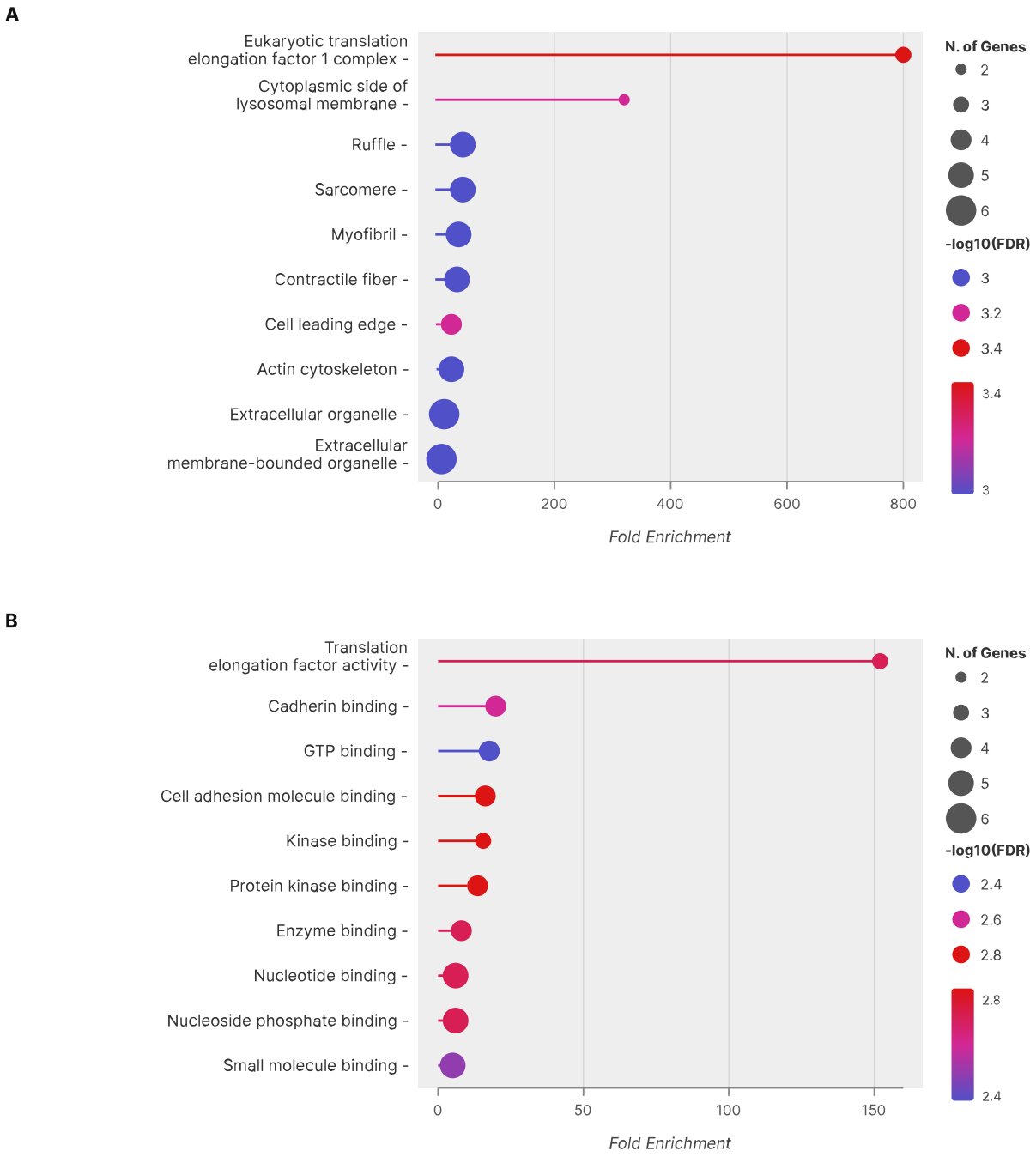


Figure 8. Fold enrichment analysis of proteins abundant in AFA method samples with T-PER buffer, "GO Cellular component" (A), and "GO Molecular function" (B).

Samples Treated with 5M Urea

Most of the significant proteins in the homogenization group were associated with nucleosome, DNA packaging complex, protein-DNA complex, and nuclear chromosome. Different extracellular components, including organelles, vesicles, and exosomes, were also enriched (**Figure 9A**). The highest fold enrichment, with strong significance, was identified for the "structural constituent of chromatin", with many proteins contributing to the enrichment (**Figure 9B**). These included the detected histone proteins (Q5TEC6; P68431; P84243; Q16695; Q71DI3), which make up the nucleosome, as well as vimentin

(P08670), which is also present in the nucleus.[35,36] UniProt analysis showed that many of the IDs were associated with different organelles, such as mitochondria- associated proteins, Q00325, O14880, P31930, P24539, and P08670, present in different mitochondrial compartments,[36–40] or calnexin (P27824), and vimentin (P08670) present in the ER.[36,41] Other significant proteins were associated with immune system activation, including four HLA class I and II histocompatibility antigens that are responsible for antigen presentation to the T cells, as well as chymase (P23946) and tryptase beta-2 (P20231), inflammatory proteins secreted by mast cells.[42,43]

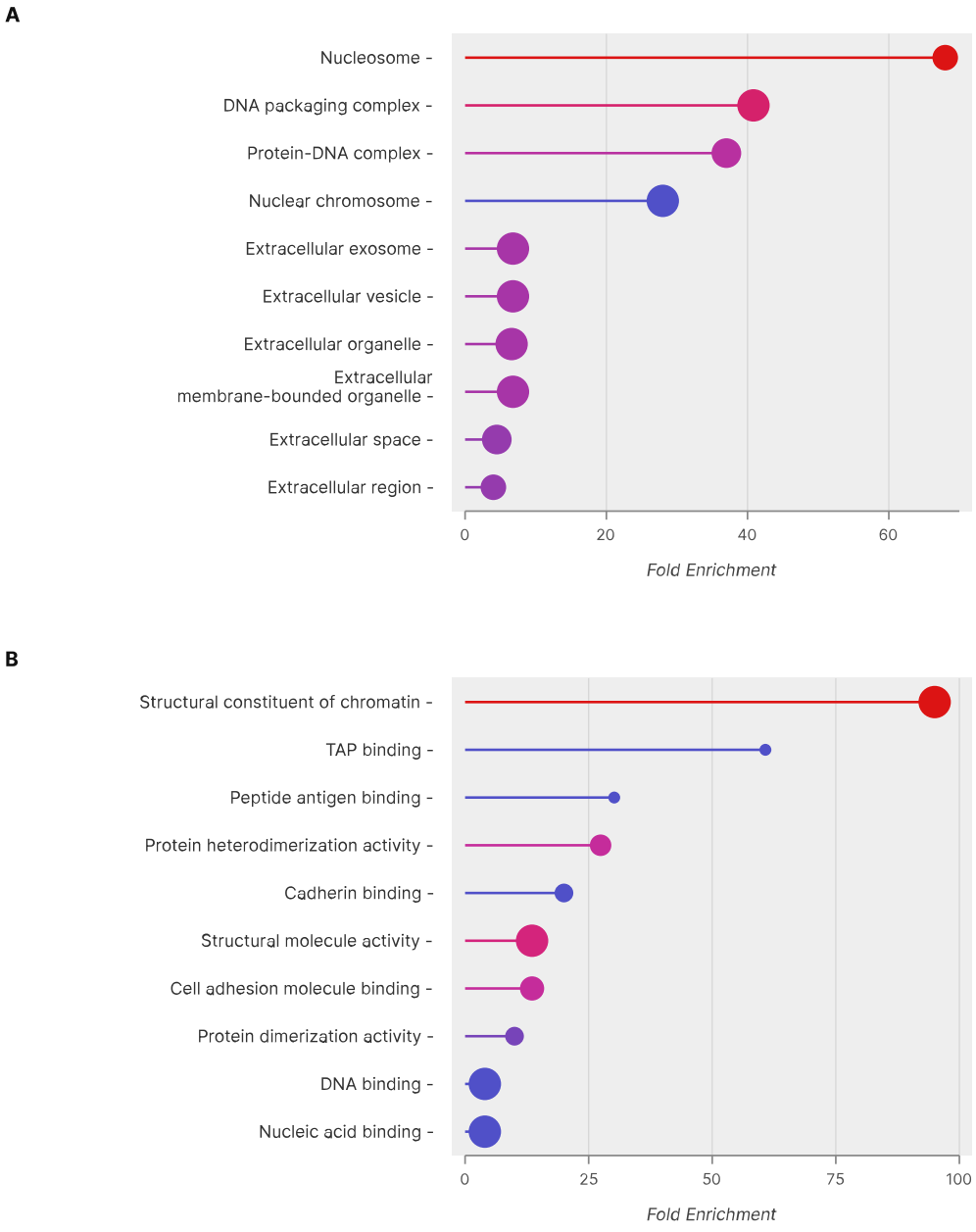


Figure 9. ShinyGO fold enrichment analysis of statistically significant proteins detected in the homogenization method with 5M urea, cellular component (A) and molecular function (B).

In the AFA sample group treated with 5M urea buffer, 12 protein IDs had increased abundance compared to the homogenization group. Most of the significant proteins were associated with protein phosphatase complexes, the spindle apparatus, and the intracellular bridge. Different extracellular components were also enriched (**Figure 10A**). The GO Molecular Function analysis showed the highest fold enrichment for "Structural constituent of cytoskeleton" (**Figure 10B**). Tubulin proteins (Q9BUF5; P07437; Q13509; P68371; Q13885; Q9BVA1; P04350; Q3ZCM7) form microtubules, which are important structures forming the mitotic spindle involved in chromosome segregation during cell division.[44] Serine/threonine-protein phosphatase 4 (P60510) is involved in microtubule organization at centrosomes and DNA repair, and is present in the cytoplasm and nucleus.[45] Like in the homogenization group, some significant protein IDs were also located within the nucleus. These included the high mobility group proteins (P26583; P09429; B2RPK0), including high mobility group protein B1 (P09429), a chromosome-binding protein and an extracellular inflammatory cytokine, as well as 26S proteasome non-ATPase regulatory subunit 8 (P48556), which is present in the nucleus and cytoplasm and is responsible for the degradation of ubiquitinated proteins.[46,47]

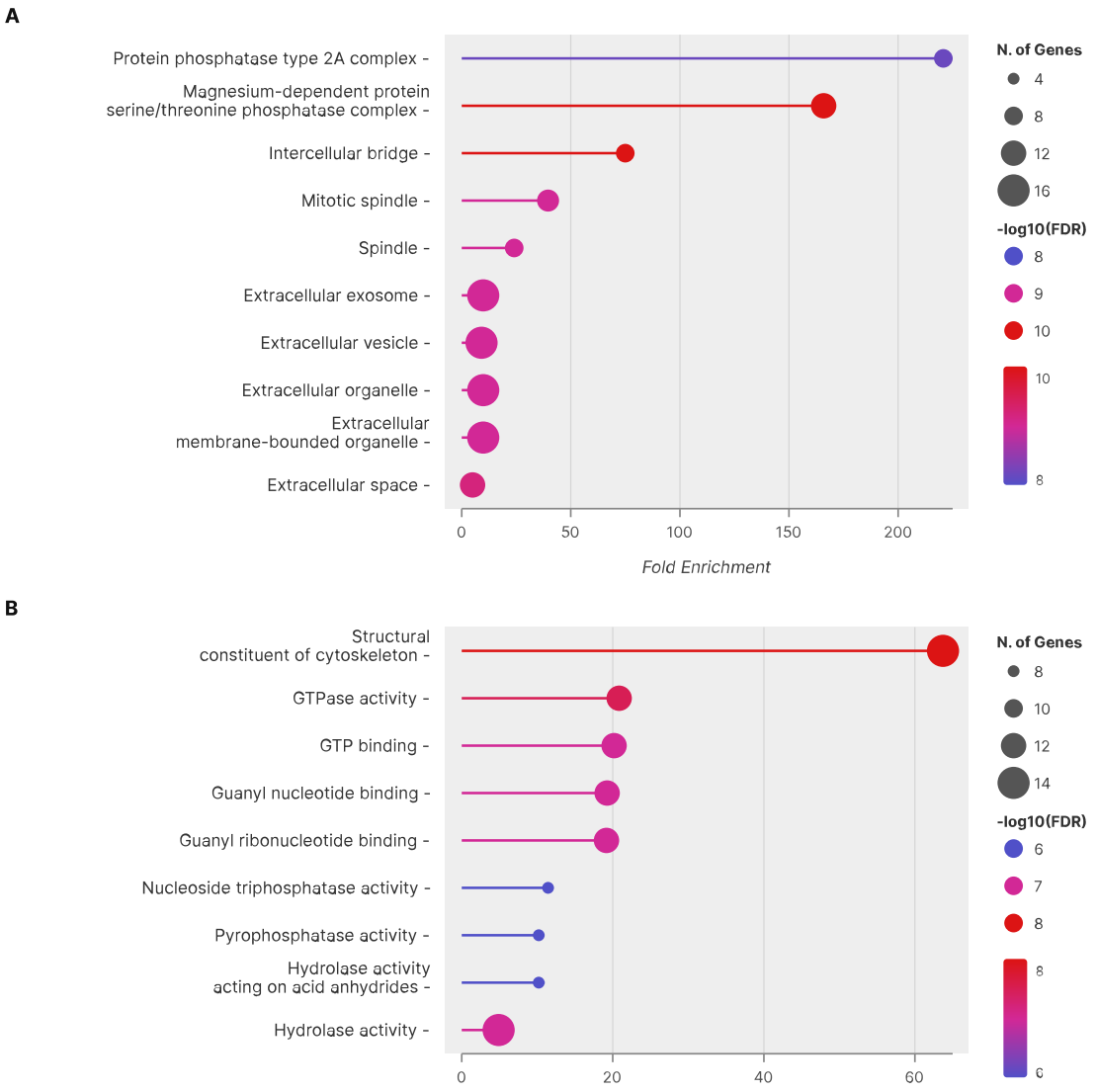


Figure 10. ShinyGO fold enrichment analysis of statistically significant proteins detected in AFA method with 5M urea, cellular component (**A**) and molecular function (**B**).

Methods that improve extraction efficiency across diverse protein classes can enhance the identification of proteins. In this context, the AFA-based extraction approach may support more consistent and efficient disruption of biological material, facilitating low-abundance protein extraction and contributing to enhanced analytical depth.

Conclusion

Although no clear trends were observed regarding the biological origin of the significantly different proteins, the results demonstrate that the use of Covaris AFA technology improved the overall number of detected protein IDs, including the number of low-abundant proteins. The origin of the significant proteins appeared to depend largely on the extraction buffer used. T-PER has been described by the manufacturer as a mild reagent with neutral pH, recommended for fibrous and collagenous tissues.[27] These characteristics may explain the higher protein extract concentrations observed with T-PER compared to 5M urea.

Both extraction buffers yielded improved results when combined with the AFA method, indicating that AFA-assisted extraction can enhance protein recovery across different lysis chemistries. Consequently, the selection of the extraction buffer for future applications should be guided by the specific protein population or biomarker targets of interest. In addition, AFA technology enhances mixing and energy transfer within the sample, which can improve the interaction between detergents, denaturants, and salts with biological material. Therefore, further investigation of additional extraction buffers would be valuable to fully optimize AFA-based workflows, as direct comparisons between conventional homogenization and AFA extraction may not always be directly equivalent.

The Covaris R230 Focused-ultrasonicator enabled precise control of temperature, acoustic power, and treatment duration during sample processing, allowing highly reproducible sample handling. Furthermore, combining AFA with the autoSP3 Bravo platform enabled a highly automated workflow with reduced manual intervention and minimized risk of processing errors. The ability to process up to 96 samples simultaneously ensured uniform processing conditions across all samples, thereby reducing experimental bias, minimizing sample-to-sample variation, and increasing the likelihood of generating consistent and reliable proteomic data.

References

1. Aslam B, Basit M, Nisar MA, Khurshid M, Rasool MH. Proteomics: Technologies and Their Applications. J Chromatogr Sci [Internet]. 2017 Feb 1;55(2):182–96. Available from: https://doi.org/10.1093/chromsci/bmw167
2. Jiang Y, Schuster D, Neely BA, Rosano GL, Volkmar N, Momenzadeh A, et al. Comprehensive Overview of Bottom-Up Proteomics Using Mass Spectrometry. ACS Measurement Science Au [Internet]. 2024;4(4):338–417. Available from: https://pubs.acs.org/doi/10.1021/acsmeasuresciau.3c00068
3. Åkesson J, Hojjati S, Hellberg S, Raffetseder J, Khademi M, Rynkowski R, et al. Proteomics reveal biomarkers for diagnosis, disease activity and long-term disability outcomes in multiple sclerosis. Nat Commun [Internet]. 2023;14(1):6903. Available from: https://doi.org/10.1038/s41467-023-42682-9
4. Allen KD, Thoma LM, Golightly YM. Epidemiology of osteoarthritis. Osteoarthritis Cartilage [Internet]. 2022;30(2):184–95. Available from: https://www.sciencedirect.com/science/article/pii/S1063458421008864
5. Zeng N, Yan ZP, Chen XY, Ni GX. Infrapatellar Fat Pad and Knee Osteoarthritis. Aging Dis. 2020;11(5):1317.
6. Duong VA, Lee H. Bottom-Up Proteomics: Advancements in Sample Preparation. Int J Mol Sci [Internet]. 2023;24(6):5350. Available from: https://www.mdpi.com/1422-0067/24/6/5350
7. Karpievitch Y V, Polpitiya AD, Anderson GA, Smith RD, Dabney AR. Liquid chromatography mass spectrometry-based proteomics: Biological and technological aspects. Ann Appl Stat [Internet]. 2010;4(4):1797–823. Available from: https://www.ncbi.nlm.nih.gov/pmc/articles/PMC3095207/
8. Dupree EJ, Jayathirtha M, Yorkey H, Mihasan M, Petre BA, Darie CC. A Critical Review of Bottom-Up Proteomics: The Good, the Bad, and the Future of This Field. Proteomes [Internet]. 2020;8(3):14. Available from: https://www.mdpi.com/2227-7382/8/3/14
9 da Costa JP, Santos PSM, Vitorino R, Rocha-Santos T, Duarte AC. How low can you go? A current perspective on low-abundance proteomics. TrAC Trends in Analytical Chemistry. 2017;93:171–82.
10. Tüshaus J, Sakhteman A, Lechner S, The M, Mucha E, Krisp C, et al. A region-resolved proteomic map of the human brain enabled by high-throughput proteomics. EMBO J. 2023;42(23).

11. Pujari GP, Mangalaparthi KK, Madden BJ, Bhat FA, Charlesworth MC, French AJ, et al. A High-Throughput Workflow for FFPE Tissue Proteomics. J Am Soc Mass Spectrom. 2023;34(7):1225–9.
12. Höring M, Krautbauer S, Hiltl L, Babl V, Sigruener A, Burkhardt R, et al. Accurate lipid quantification of tissue homogenization requires suitable sample concentration, solvent composition, and homogenization procedure—a case study in murine liver. Metabolites [Internet]. 2021 Jun 1 [cited 2025 Apr 28];11(6):365. Available from: https://www.mdpi.com/2218-1989/11/6/365/htm
13. Emanuel KS, Luojiao H, Mirella J. J. H, Javier SM, Frank Z, Ron M. A. H, et al. Patient-responsive protein biomarkers for cartilage degeneration and repair identified in the infrapatellar fat pad. Expert Rev Proteomics [Internet]. 2024 Dec 1;21(12):563–73. Available from: https://doi.org/10.1080/14789450.2024.2438774
14. Sleczka, B. G., Levesque, P. C., Adam, L. P., Olah, T. V., & Shipkova, P. (2020). LC/MS/MS-based quantitation of pig and human S100A1 protein in cardiac tissues: Application to gene therapy. Analytical Biochemistry, 602, 113766. https://doi.org/10.1016/j.ab.2020.113766
15. Soporan MA, Pralea IE, Iacobescu M, Moldovan RC, Alkhzouz C, Miclea D, et al. Salivary Proteome Insights: Evaluation of Saliva Preparation Methods in Mucopolysaccharidoses Research. Biomedicines. 2025 Mar 1;13(3).
16. Nanduri B, Shack LA, Rai AN, Epperson WB, Baumgartner W, Schmidt TB, et al. Use of focused ultrasonication in activity-based profiling of deubiquitinating enzymes in tissue. Anal Biochem [Internet]. 2016;515:9–13. Available from: https://www.sciencedirect.com/science/article/pii/S0003269716303050
17. Dhabaria A, Cifani P, Reed C, Steen H, Kentsis A. A High-Efficiency Cellular Extraction System for Biological Proteomics. J Proteome Res [Internet]. 2015 Aug 7;14(8):3403–8. Available from: https://doi.org/10.1021/acs.jproteome.5b00547
18. Müller T, Kalxdorf M, Longuespée R, Kazdal DN, Stenzinger A, Krijgsveld J. Automated sample preparation with SP 3 for low-input clinical proteomics . Mol Syst Biol [Internet]. 2020 Jan 16 [cited 2025 Apr 28];16(1):9111. Available from: https://doi.org/pdf/10.15252/msb.20199111?download=true
19. Hughes CS, Moggridge S, Müller T, Sorensen PH, Morin GB, Krijgsveld J. Single-pot, solid-phase-enhanced sample preparation for proteomics experiments. Nat Protoc [Internet]. 2019 Jan 1 [cited 2025 May 2];14(1):68–85. Available from: https://pubmed.ncbi.nlm.nih.gov/30464214/
20. Varnavides G, Madern M, Anrather D, Hartl N, Reiter W, Hartl M. In Search of a Universal Method: A Comparative Survey of Bottom-Up Proteomics Sample Preparation Methods. J Proteome Res [Internet]. 2022 Oct 7;21(10):2397–411. Available from: https://doi.org/10.1021/acs.jproteome.2c00265
21. Sielaff M, Kuharev J, Bohn T, Hahlbrock J, Bopp T, Tenzer S, et al. Evaluation of FASP, SP3, and iST Protocols for Proteomic Sample Preparation in the Low Microgram Range. J Proteome Res [Internet]. 2017 Nov 3;16(11):4060–72. Available from: https://doi.org/10.1021/acs.jproteome.7b00433
22. Demichev V, Messner CB, Vernardis SI, Lilley KS, Ralser M. DIA-NN: neural networks and interference correction enable deep proteome coverage in high throughput. Nat Methods [Internet]. 2020;17(1):41–4. Available from: https://doi.org/10.1038/s41592-019-0638-x
23. Zhang F, Ge W, Huang L, Li D, Liu L, Dong Z, et al. A Comparative Analysis of Data Analysis Tools for Data-Independent Acquisition Mass Spectrometry. Molecular & Cellular Proteomics [Internet]. 2023;22(9):100623. Available from: https://www.sciencedirect.com/science/article/pii/S1535947623001342
24. Bowler-Barnett, E., Fan, J., Luo, J., Magrane, M., Martin, M., & Orchard, S. (2023). UniProt and Mass Spectrometry-Based Proteomics—A 2-Way working relationship. Molecular & Cellular Proteomics, 22(8), 100591. https://doi.org/10.1016/j.mcpro.2023.100591
25. Tyanova, S., Temu, T., Sinitcyn, P., Carlson, A., Hein, M. Y., Geiger, T., Mann, M., & Cox, J. (2016). The Perseus computational platform for comprehensive analysis of (prote)omics data. Nature Methods, 13(9), 731–740. https://doi.org/10.1038/nmeth.3901
26. Stability of urea in solution and pharmaceutical preparations - PubMed [Internet]. [cited 2025 May 2]. Available from: https://pubmed.ncbi.nlm.nih.gov/25043489/
27. T-PERTM Tissue Protein Extraction Reagent [Internet]. [cited 2025 May 16]. Available from: https://www.thermofisher.com/order/catalog/product/78510
28. Ma C, Li Y, Li J, Song L, Chen L, Zhao N, et al. Comprehensive and deep profiling of the plasma proteome with protein corona on zeolite NaY. J Pharm Anal [Internet]. 2023;13(5):503–13. Available from: https://www.sciencedirect.com/science/article/pii/S2095177923000631
29. Barreto G, Senturk B, Colombo L, Brück O, Neidenbach P, Salzmann G, et al. Lumican is upregulated in osteoarthritis and contributes to TLR4-induced pro-inflammatory activation of cartilage degradation and macrophage polarization. Osteoarthritis Cartilage [Internet]. 2020 Jan 1 [cited 2025 May 14];28(1):92–101. Available from: https://pubmed.ncbi.nlm.nih.gov/31715293/
30. SOD3 - Extracellular superoxide dismutase [Cu-Zn] - Homo sapiens (Human) | UniProtKB | UniProt [Internet]. [cited 2025 May 14]. Available from: https://www.uniprot.org/uniprotkb/P08294/entry
31. Maruyama T, Nara K, Yoshikawa H, Suzuki N. Txk, a member of the non-receptor tyrosine kinase of the Tec family, forms a complex with poly(ADP-ribose) polymerase 1 and elongation factor 1α and regulates interferon-γ gene transcription in Th1 cells. Clin Exp Immunol [Internet]. 2007 Jan [cited 2025 May 14];147(1):164–75. Available from: https://pubmed.ncbi.nlm.nih.gov/17177976/

32. Dixon RDS, Arneman DK, Rachlin AS, Sundaresan NR, Costello MJ, Campbell SL, et al. Palladin Is an Actin Cross-linking Protein That Uses Immunoglobulin-like Domains to Bind Filamentous Actin*. Journal of Biological Chemistry [Internet]. 2008;283(10):6222–31. Available from: https://www.sciencedirect.com/science/article/pii/S0021925820572001
33. Acconcia F, Barnes CJ, Singh RR, Talukder AH, Kumar R. Phosphorylation-dependent regulation of nuclear localization and functions of integrin-linked kinase. Proc Natl Acad Sci U S A [Internet]. 2007 Apr 17 [cited 2025 May 14];104(16):6782–7. Available from: https://www.pnas.org/doi/pdf/10.1073/pnas.0701999104
34. Prechova M, Korelova K, Gregor M. Plectin. Current Biology [Internet]. 2023;33(4):R128–30. Available from: https://www.sciencedirect.com/science/article/pii/S0960982222019984
35. Bano D, Salomoni P, Ehninger D, Nicotera P. The histone code in dementia: Transcriptional and chromatin plasticity fades away. Curr Opin Pharmacol [Internet]. 2021 Oct 1 [cited 2025 May 15];60:117–22. Available from: https://www.sciencedirect.com/science/article/pii/S1471489221001089
36. VIM - Vimentin - Homo sapiens (Human) | UniProtKB | UniProt [Internet]. [cited 2025 May 15]. Available from: https://www.uniprot.org/uniprotkb/P08670/entry
37. SLC25A3 - Solute carrier family 25 member 3 - Homo sapiens (Human) | UniProtKB | UniProt [Internet]. [cited 2025 May 15]. Available from: https://www.uniprot.org/uniprotkb/Q00325/entry
38. MGST3 - Glutathione S-transferase 3, mitochondrial - Homo sapiens (Human) | UniProtKB | UniProt [Internet]. [cited 2025 May 15]. Available from: https://www.uniprot.org/uniprotkb/O14880/entry
39. UQCRC1 - Cytochrome b-c1 complex subunit 1, mitochondrial - Homo sapiens (Human) | UniProtKB | UniProt [Internet]. [cited 2025 May 15]. Available from: https://www.uniprot.org/uniprotkb/P31930/entry
40. ATP5PB - ATP synthase peripheral stalk subunit b, mitochondrial - Homo sapiens (Human) | UniProtKB | UniProt [Internet]. [cited 2025 May 15]. Available from: https://www.uniprot.org/uniprotkb/P24539/entry
41. CANX - Calnexin - Homo sapiens (Human) | UniProtKB | UniProt [Internet]. [cited 2025 May 15]. Available from: https://www.uniprot.org/uniprotkb/P27824/entry
42. Atiakshin D, Buchwalow I, Tiemann M. Mast cell chymase: morphofunctional characteristics. Histochem Cell Biol [Internet]. 2019 Oct 1 [cited 2025 May 14];152(4):253–69. Available from: https://link.springer.com/article/10.1007/s00418-019-01803-6
43. Payne V, Kam PCA. Mast cell tryptase: a review of its physiology and clinical significance. Anaesthesia [Internet]. 2004 Jul 1 [cited 2025 May 14];59(7):695–703. Available from: https://doi.org/pdf/10.1111/j.1365-2044.2004.03757.x
44. Ferreira LT, Figueiredo AC, Orr B, Lopes D, Maiato H. Dissecting the role of the tubulin code in mitosis. Methods Cell Biol [Internet]. 2018 Jan 1 [cited 2025 May 15];144:33. Available from: https://pmc.ncbi.nlm.nih.gov/articles/PMC6402544/
45. PPP4C - Serine/threonine-protein phosphatase 4 catalytic subunit - Homo sapiens (Human) | UniProtKB | UniProt [Internet]. [cited 2025 May 15]. Available from: https://www.uniprot.org/uniprotkb/P60510/entry
46. Yuan S, Liu Z, Xu Z, Liu J, Zhang J. High mobility group box 1 (HMGB1): a pivotal regulator of hematopoietic malignancies. Journal of Hematology & Oncology 2020 13:1 [Internet]. 2020 Jul 13 [cited 2025 May 15];13(1):1–19. Available from: https://jhoonline.biomedcentral.com/articles/10.1186/s13045-020-00920-3
47. PSMD8 - 26S proteasome non-ATPase regulatory subunit 8 - Homo sapiens (Human) | UniProtKB | UniProt [Internet]. [cited 2025 May 15]. Available from: https://www.uniprot.org/uniprotkb/P48556/entry

Covaris® a PerkinElmer Company

Tel: +1 781-932-3959 info@covaris.com

Learn more by scanning the QR code

Covaris® and the Covaris logo are trademarks of Covaris, LLC. All other trademarks, service marks, and trade names are the property of their respective owners. Unauthorized use of Covaris trademarks is strictly prohibited. Information subject to change without notice. www.covaris.com. 2026© Covaris, LLC. mkt_5564_RevA_October2026

US: +1 781.932.3959
customerservice@covaris.com

EU: +44 (0)845 872 0100
emeacustomerservice@covaris.com

Applications
applicationsupport@covaris.com

Service and Support
techsupport@covaris.com